Effective Utilization of Renewable Energy Sources To Generate and Control Power in Ac Isolated Micro Grid

D. Tulasi Phani Swami, T. Kranti Kiran

Abstract: ***This paper presents new technology to regulate the power from energy resources existing on our requirements in micro grid (or) load balances. Power control by using battery banks in existing power electronic converter is employed to form AC grid GFC (grid former converter), associate energy source supported to a wind turbine and solar energy. To generate the power with its respective power electronics converter GSC (grid supplier converter) and therefore utilizes by power consumers. The main objective of this proposed strategy is to generate the power from wind turbine (WT), photovoltaic (PV) generation and to regulate the power distributed through battery banks by keeping the ESS from over charge (or) over discharge conditions through regulating the voltage terminals by controlling the power generated by wind and solar. This is done without using dump loads or any physical communication among the power electronic converters or the individual energy source controllers. The electrical frequency of the micro grid is used to inform the power sources and their respective converters about the amount of power that they need to generate in order to maintain the battery-bank charging voltage below or equal its maximum allowable limit. The primary merit for proposal method is to make the generated power at normal cost for military purpose and development progress.***

Keywords: Battery Banks, Power Electronics Converters, Controllers, Renewable Energy Sources (RES'S), State of Charge (SOC).

I. INTRODUCTION

Presently in a modern situation there is no access to power electricity produced to remote located areas such as in island areas, that places are used in renewable energy resources particularly solar and wind. These energy resources used in form isolated micro grid to meet local energy needs [1], [2]. The supply of electricity to these communities in several developing countries, in general, still done in a precarious way using diesel generators that operate for 3-4h day[2]. The MG is introduced by (CERTS) the consortium for electric reliability technology solutions. Renewable energy sources are fuel cells, wind turbine and solar energy systems .This energy maintained to battery banks with power electronic devises (i.e. batteries, supper capacitors and fly wheels) and consumer loads that could operate using automatically devises form. MG are often considered as a local grid with multiple distributed generators (DGs), ESS, and loads, ready to operate either in grid connected or islanded mode. Microgrid will provide clean, reliable and uninterruptible power.

Revised Version Manuscript Received on December 09, 2017.

D. Tulasi Phani Swami, PG Scholar, Department of Electronics and Electrical Engineering, Sir C R Reddy College of Engineering, Eluru (A.P), India. E-mail: tulasiswami@gmail.com

T. Kranti Kiran, Assistant Professor, Department of Electronics and Electrical Engineering, Sir C R Reddy College of Engineering, Eluru (A.P), India. E-mail: kratikiran.mtech@gmail.com

II. PROPOSED MODELING OF MICRO GRID

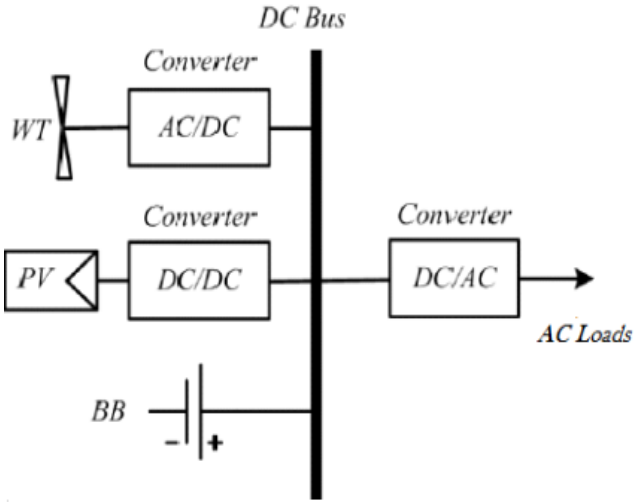

Fig.1 Proposed Model of Microgrid

The coordinated active power management strategy should take under consideration status of all microgrid components such as the SOC of ESS, power offered from the Wind, PV systems by using battery banks, and demand of power consumption. The applications of MG's will vary in storage, advanced controls, size in Mega Watts, generation resource sorts, microgrid worth proposition. The MG's offers Energy security, grid independence capability and ensure energy supply for essential loads utilizing on site generation.

MG has two typical operational modes

1. Grid Connected Mode
2. Islanded Mode Operation

A. Grid Connected Mode:

Grid- connected mode and islanded mode [6]. Below traditional circumstances, the MG operates in grid-connected mode that is connected to the upstream grid, being either partly equipped from it or injecting some quantity of power. The power Stream MG is connected to the distribution system through wind and solar energy. The energy stored in batteries which are sodium nickel chloride, lithium ion battery, lead acid batteries to maintain grid operation mode.

B. Islanded Mode Operation:

Islanded mode operation is distribution system disconnected to the main grid, connected to micro grid continuous supply will be provided.

Published By:
Blue Eyes Intelligence Engineering
& Sciences Publication Pvt. Ltd.

III. SYSTEM DESCRIPTION

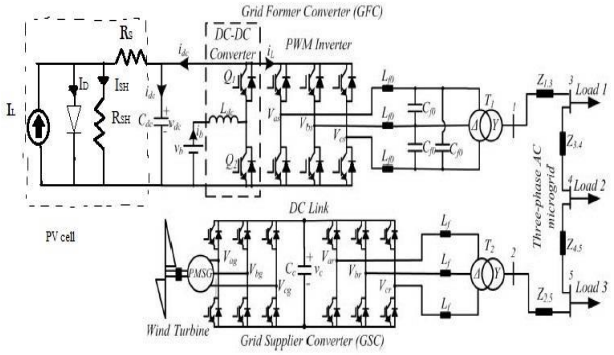

Fig: 2. Simplified Diagram of Studied Micro Grid

As shown in above figure simplified that the control strategy proposed in this paper important terms are consist of a GFC , a GSC and battery bank. mainly used in wind turbine side (PMSG) permanent magnet coupled to synchronous generator depending up on the based micro grid size, The GFC is a bidirectional converter formed by a pulse width modulation (PWM) three phase inverter and DC-DC converter this is the two operation modes are performed that is buck mode and boost mode that works in buck mode when the battery bank is under charge or in a boost mode when it is under discharge. the PWM inverter controls the magnitude and frequency of the microgrid voltage while the two modes are used to control the voltage at the dc bus capacitor(C_{dc}) which is the dc bus voltage as well as the charging and discharging of the battery bank. The GSC is used to control the power generated by renewable energy source .the converter is worked by a back to back topology [12] .it has[TSI] is the turbine-side inverter, and grid-side PWM inverter(GSI), TSI is used to control the turbine power generated by the wind turbine based on a maximum power point tracker, GSI is used to control the DC-link voltage of the back to back topology.

IV. GRID FORMER CONVERTER

A. Control of the Microgrid Voltage and Frequency

The MG voltage controller uses synchronous dq reference frame, with an inner current loop and an outer voltage loop. Using droop control strategy the frequency and voltage reference values are calculated as functions of the active and reactive power severally at the grid former converter terminals. The dq model of the LC filter in the delta side of transformer T1as shown in figure: 3 below

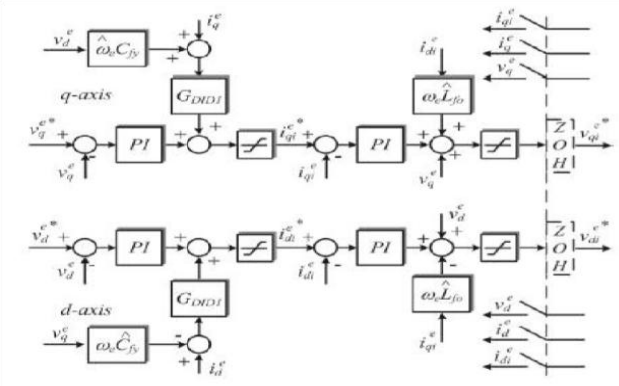

Fig: 3. Micro Grid Voltage Controller

where R_{f0} the equivalent series resistance of the filter inductor L_{f0}; ω_e is the micro grid frequency radians per second, "e" denotes variable in the dq synchronous reference frame, i^e_d and i^e_q are the dq currents in the delta side transformer T1; C_{fy} is the per phase equivalent capacitance of the LC filter and is equal to $3C_{f0}$ during this paper use the operator p = *d/dt*. The voltage reference values for the voltage controllers will be constant, typically adequate to the nominal value of the microgrid voltage, or will be calculated based on a droop control strategy. During this paper, the voltage reference was mounted in 220 V (*rms* line voltage within the delta side of T1). By considering that the dq synchronous reference frame is aligned with the microgrid voltage vector, the reference values of the dq voltages are v_d^{e*}= 0V, and v_q^{e*}=179.6V. The frequency reference value is calculated by using the power control strategy.

B. Control of Bi-Directional DC-DC Converter

The dc–dc converter (in GFC) is employed to regulate the voltage in the capacitor C . The action of the controller of the dc–dc converter will be considered comparable to connecting a controlled voltage source, with mean valueV_{ct}, between the *xy* Terminals of the converter circuit, as shown in Fig. 7(a) and (b). If the losses within the converter aren't considered, the voltage on C_{dc} depends solely on the difference between the power at the BB terminals (P_b) and (P_{inv}) that is the power at the terminals of the delta side of the isolation transformer T1, ω_{dc}= $v_{dc}{}^2$

$$\frac{1}{2}C_{dc}\frac{dv_{dc}^2}{dt} = \frac{1}{2}C_{dc}\frac{dw_{dc}}{dt} = P_b - P_{inv} \qquad (1)$$

V. GRID SUPPLIER CONVERTER

A. Control of the Injected Current in the Microgrid and the Voltage at the DC Bus

In this paper to control the dc bus voltage, the GSI of the GSC (see Fig.3) of the back-to-back topology is employed. The inner current loop of this controller is used to regulate the injected current within the microgrid. The current controller is enforced in a dq synchronous reference frame aligned with the microgrid positive sequence voltage vector. By employing a synchronous phase-locked loop (PLL) converter variable synchronization is completed which has a second-order resonant filter tuned for the fundamental frequency of the microgrid. As shown in Fig.3. If the losses within the GSI and within the inductor lf are neglected, the variation of the energy stored within the capacitor C_c is equal to the difference between the active powers received from the MG (P_s) and therefore the active power generated by the wind turbine (P_g). Using the convention of Fig.3, this could be expressed as in.

$$\frac{1}{2}C_{dc}\frac{dw_c^2}{dt} = P_s - P_g; w_c = v_c^2 \qquad (2)$$

For a dq synchronous reference frame aligned with the microgrid voltage vector, it follows that e^e_{ds}= 0. Therefore, Ps is adequate to (3/2)$i_{qs}{}^e$,

With E_s being the magnitude of the part voltage, thought-about constant in this application. By defining K_c adequate to $(3/2E_s)$, the dynamic equation for the capacitor C_c is presented in

$$\frac{dw_c}{dt} = \frac{2}{c_c}(K_c i_{qs}^e - P_g) \qquad (3)$$

B. Control of the Wind Turbine Generated Power

The power generated control strategy uses the TSI to regulate the torque of the PMSG, leading to the control of its generated power. The torque control relies on the control of the generator current. The TSI current controller is implemented on a synchronous dq reference frame aligned with the rotor of the wind turbine generator. Based on the conventions adopted in this work, the d-axis current component (i_d) of the generator is controlled to be zero. Thus, in steady state, the generator torque (T_g) is proportional to its q-axis current reference component (i_q^*), as shown in (4) [14], wherever kg is given by (5), P is the number of generator poles, and λ_{mf} is that the generator permanent magnet flux

$$T_g = K_g i_q^* \qquad (4)$$

$$K_g = \left(\frac{3}{2}\right)\left(\frac{P}{2}\right)\lambda_{mf} \qquad (5)$$

The mechanical torques of a wind turbine as a function of the rotational speed of the wind turbine (ω_R) for different wind speeds. When the wind turbine works on its point of maximum power production, the mechanical torque (T_M) made is proportional to the square. Ofω_R, as indicated by T_{Motm}.where K_{Tot} could be a constant that depends on the physical and operational characteristics of the turbine and on the air density. The value of K_{Totm} could also be obtained by experimentation or from computational simulations, based on mathematical models of the turbine [15].

$$T_M = T_{Motm} = K_{Totm} K_{Totm} \omega_R^2 \qquad (6)$$

One possible MPPT algorithmic rule for the turbine is often implemented by making the generator toque curve coincide with the optimum curve of the turbine mechanical torque ($T_g = T_{Motm}$) [16]. As a result, the reference value for the q-axis generator current (i_q^*) is given by

$$i_q^* = (K_{Totm}/K_g)\omega_R^2 = K_{iq}\omega_R^2 \qquad (7)$$

C. DC-DC Converter

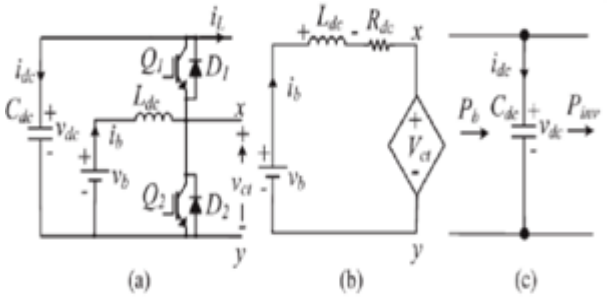

Fig: 4. DC–DC converter average model: (a) Original circuit, (b) equivalent average circuit of inductor and battery bank, and (c) average model of the bus dc.

D. Equivalent Circuit of Lead acid Battery

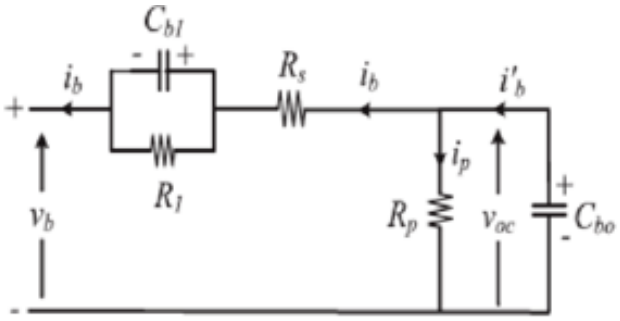

Fig. 5. Lead–Acid Battery Equivalent Circuit.

On this case, there aren't any restrictions concerning the amount of power that may be generated, and therefore the existing renewable energy sources will function on their maximum power point. Obviously, this is true as long as the battery bank has been designed with sufficient capability to absorb all the power that the renewable sources will produce at a given instant.

$$f_0 - k_p P_{inv} \qquad (8)$$

The amount of power that needs to be reduced from the maximum power that each} source is ready to supply at every moment has a direct relation to the frequency difference Δf = f −f_{max}. The values of f_0 and $\pm\Delta f_{max}$ adopted during this work are 60 Hz and ± 0.60 Hz in order that the frequency range of the MG is between 59.4 Hz (f_{min}) and 61.2 Hz (f_{max} + Δf_{max}), which meets the European standard EM50160 [18].

$$f = f_{max} + \Delta f(v_b, P_g, P_{inv}) \qquad (9)$$

E. Tuning of the Battery Bank Terminal Voltage Controller

The standardization of the PI controller shown in Fig.6. takes into account the dynamic of the battery bank. One possible model for lead–acid batteries is shown in Fig.5 [19].

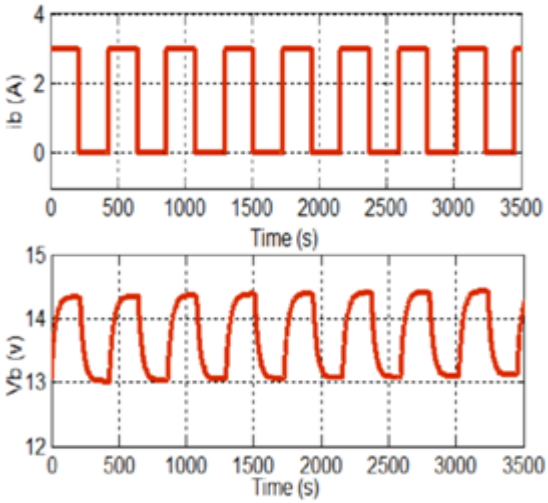

Fig.6. Experimental Waveforms During the Tests with a 30-Ah 12-V Lead–Acid Battery. (a) Current. (b) Voltage.

Published By:
Blue Eyes Intelligence Engineering
& Sciences Publication Pvt. Ltd.

In this Fig.5,v_{oc} is that the battery open circuit voltage, R is that the equivalent series internal resistance, R_1 and C_{b1} are used to model the over- or under voltage that happens once the battery is charging or discharging, R_p is that the resistance due the natural losses, and C_{b0} models the battery capacity to storage energy. Normally, the natural losses occur terribly slowly, therefore the effect of $_p$ will be disregarded for the aim of this work.

The calculable parameters obtained after a charging cycle, once the voltage of the battery is approximately 14.3 V are R_s = 8.7 mΩ, R_1 = 431.40 mΩ, C_{b1}= 64.93 F, and C_b = 49, 091.00

VI. SIMULATION RESULTS

Average speed of 8.5 m/s, ω = 2π/t , and tW= 120 s VW= 8.5+ 0.6 sin (ωt) + 0.6 sin (3.5 ωt)+0.3 sin (12.35 ωt) +0.06 sin (35 ωt)

A. Results with Constant Wind Speed

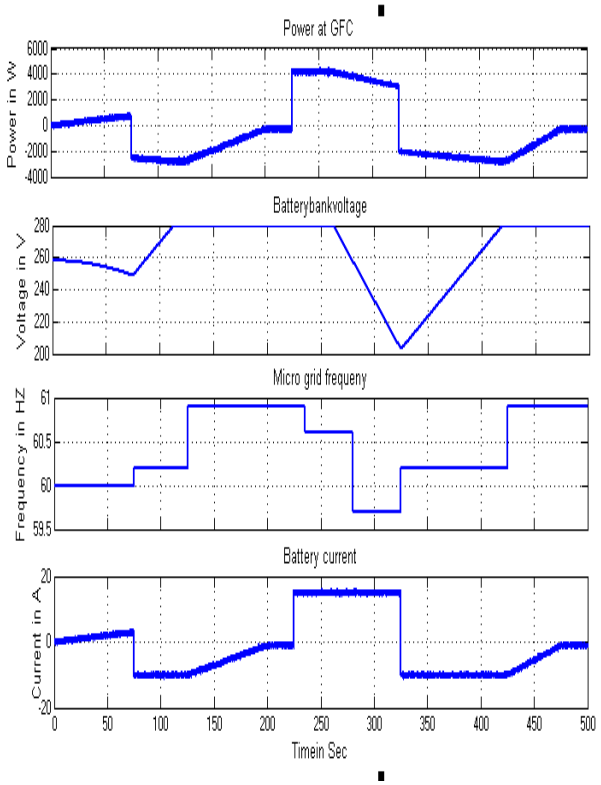

Fig.7.Constant wind Speed of 9.2 m/s: (a) Power at the GFC Terminals, (b) Battery Bank Voltage, (c) Microgrid Frequency, and (d) Battery Current.

Fig.7 shows the action of the proposed control strategy over the battery bank voltage and also the MG frequency once the battery bank is fully charged and also the wind turbine is able to generate power. In this experiment, the wind speed was considered constant and adequate to 9.2 m/s. Before the tests, the battery bank was fully charged (before the time of 0 s in Fig.7), and its open circuit voltage is 258 V. At the instant of 0 s, the GFC is turned on, and also the MG is at no load, supplying just the system losses. Until t1, the MG remains at no load, and its frequency is kept constant [see Fig.7(c)] following (8). no load, and its frequency is kept constant [see Fig.7(c)] following (8). At instant t1, the GSC is turned on, starting to inject the wind turbine power (4.5 kilowatt at GFC terminals) into the MG. Because the system is at no load, this power goes to the battery bank [see battery current in Fig.8(d)]. Whose voltage will increase, reaching its maximum value (280 V) at time t2. At this instant, the power controller begins to act, keeping the battery bank voltage at 280 V. The controller keeps the frequency on top of $fmax$ = 60.6 Hz. As a result, the generated power is reduced [see Fig.7(a)] to keep the BB voltage under control. At instant t3, a load of 7.05 kilowatt is connected to the microgrid

B. Results with Variable Wind Speed

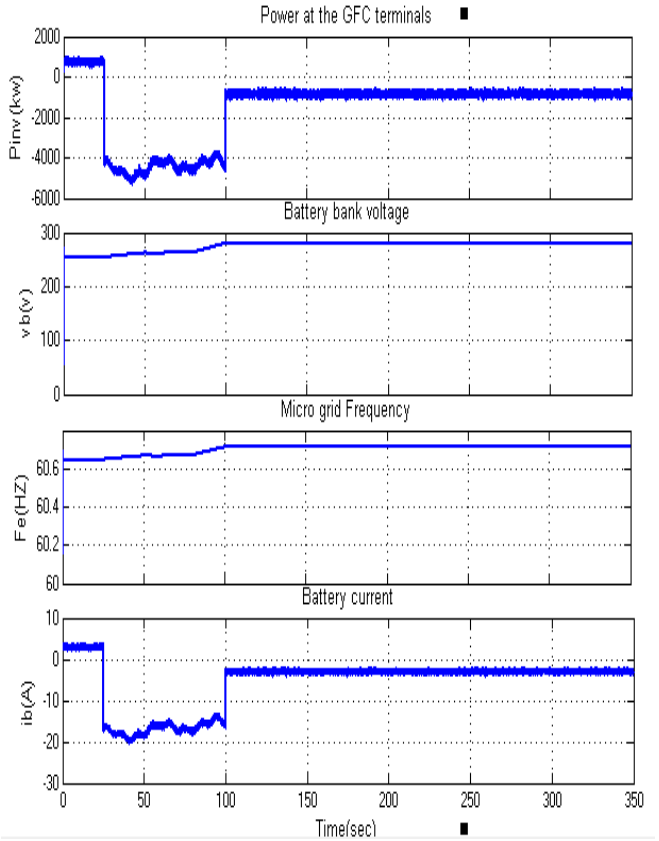

Fig. 8. Variable Wind Speed: (a) Power at the GFC Terminals, (b) Voltage, (c) Microgrid Frequency, and (d) Battery Current.

Fig.8. shows the system behavior for variable wind speed. The wind speed was synthesized in the wind turbine emulator based on the model presented in this model, the wind speed (V_w) is with an average speed of 8.5 m/s, ω = 2π/t_w , and t_w= 120 s V_W = 8.5+ 0.6 sin (ωt) + 0.6 sin (3.5 ωt)+0.3 sin (12.35 ωt) +0.06 sin (35 ωt) (14) ,the microgrid is functioning with no load, supplying only the system losses, and therefore the GSC is turned off before the instant t1. At instant t1, the GSC is turned on, and power flows to the battery bank, as shown in Fig.11.(a) and (d). Its voltage begins to increase until it reaches 280 V at instant t2 [see Fig. 11(b)]. At this instant, the power controller begins to act, reducing the generated power in order to keep the battery bank voltage under control with mean value approximately equal to 280 V.

C. Results with Constant Speed When a PV cell Connected to the MG

Published By:
Blue Eyes Intelligence Engineering
& Sciences Publication Pvt. Ltd.

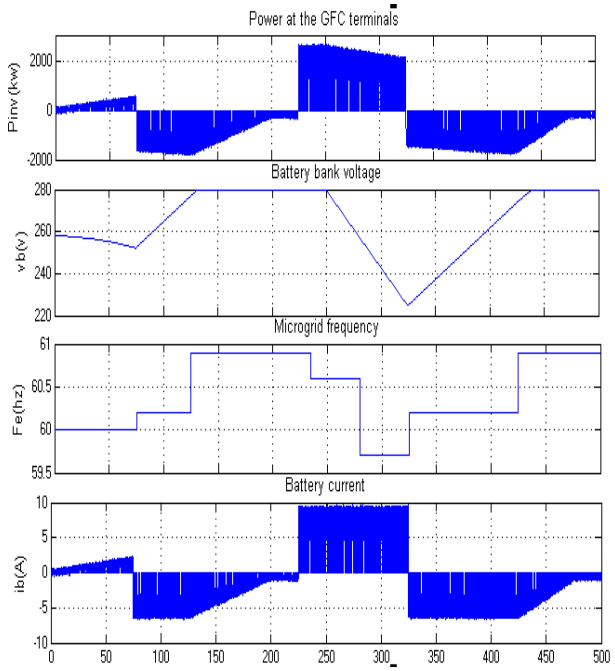

Fig. 9. Constant wind Speed of 9.2 m/s &PV cell: (a) Power at the GFC Terminals, (b) Battery Bank Voltage, (c) Microgrid Frequency, and (d) Battery Current.

while a lot of complete description of autonomous active power control in full range of SOC, and its implementation taking into consideration the ESS and PV system prime sources are self- addressed. Battery bank system is employed because the ESS which fixes bus frequency and compensates power imbalance between power generation and consumption. Every PV system is employed to supply renewable energy to the microgrid. Fig.9 shows the system at constant wind speed with the connection of PV cell with constant wind speed as 8.5 m/s, snubber resistance Rs=*500* Ω, snubber capacitance $Cs=25*e-10$ F, and as the forward voltage as100V, and resistance in parallel to the diode is 10K Ω, by simulating this model that we achieved these results.

VII. CONCLUSION

This paper presented a strategy to control the generated power in order to keep the charging voltage battery banks under control in stand-alone microgrids with distributed renewable energy sources. This strategy does not need wired communication between the distributed renewable sources nor dump loads to dissipate the surplus of generated power in the microgrid. These technical advantages make the proposed strategy a promising tool to increase the reliability and viability of the renewable power generation system installed in isolated and remote communities and minimal cost we can arrange quality power at a remote location for military purpose and development progress.. Although a wind turbine has been used to demonstrate the validity of the proposed strategy, it is also valid regardless of the power source existing in the isolated microgrid. The proposed strategy calculates the amount of power that must be generated at each time by each source in order to keep the balance of energy into the microgrid. In other words, the sum of the generated, consumed, and stored energy must always be zero all the time.

REFERENCES

1. L. A. de S. Ribeiro, O. R. Saavedra, S. L. de Lima, and J. G. de Matos, "Isolated micro-grid with renewable hybrid generation: The case of Lençóis island," IEEE Trans. Sustain. Energy, vol. 2, no. 1, pp. 1–11, Jan. 2011.
2. L. A. de S. Ribeiro, O. R. Saavedra, S. L. de Lima, and J. G. de Matos, "Making isolated renewable energy systems more reliable," Renew. Energy, vol. 45, pp. 221–231, Sep. 2012.
3. J. G. de Matos, L. A. de S. Ribeiro, and E. C. Gomes, "Power control in AC autonomous and isolated microgrids with renewable energy sources and energy storage systems," in Proc. IEEE IECON, 2013, pp. 1827–1832.
4. N. Mendis, K. M. Muttaqi, S. Pereira, and M. N. Uddin, "A novel control strategy for stand-alone operation of a wind dominated RAPS system," in Proc. IEEE IAS Annu. Meeting, 2011, pp. 1–8.
5. J. Chen, J. Cheng, C. Gong, and X. Deng, "Energy management and power control for a stand-alone wind energy conversion system," in Proc. IEEE IECON, 2012, pp. 989–994.
6. M. J. Erickson and R. H. Lasseter, "Integration of battery storage element in a CERTS microgrid," in Proc. IEEE ECCE, 2010, pp. 2570–2577.
7. J. Rocabert, J. A. Luna, F. Blaabjerg, and P. Rodrígues, "Control of power converters in ac microgrids," IEEE Trans. Power Electron., vol. 27, no. 11, pp. 4734–4749, Nov. 2012.
8. Jin, P. Wang, J. Xiao, Y. Tang, and F. H. Choo, "Implementation of hierarchical control in dc microgrids," IEEE Trans. Ind. Electron., vol. 61, no. 8, pp. 4032–4042, Feb. 2014.
9. X. Lu, K. Sun, J. M. Guerrero, J. C. Vasquez, and L. Huang, "State-ofcharge balance using adaptive droop control for distributed energy storage systems in dc microgrid applications," IEEE Trans. Ind. Electron., vol. 61, no. 6, pp. 2804–2815, Jun. 2014.
10. M. A. Abusara, J. M. Guerrero, and S. M. Sharkh, "Line-interactive UPS for microgrids," IEEE Trans. Ind. Electron., vol. 61, no. 3, pp. 1292–1300, Mar. 2014.
11. J. M. Guerrero, P. X. Loh, T.-L. Lee, and M. Chandorkar, "Advanced control architectures for intelligent microgrids–Part II: Power quality, energy storage, ac/dc microgrids," IEEE Trans. Ind. Electron., vol. 60, no. 4, pp. 1263–1270, Apr. 2013.
12. Z. Chen, J. M. Guerrero, and F. Blaabjerg, "A review of the state of art of power electronics for wind turbines," IEEE Trans. Power Electron., vol. 24, no. 8, pp. 1859–1875, Aug. 2009.
13. M. Ciobotaru, "Reliable grid condition detection and control of singlephase distributed power generation systems," Ph.D. dissertation, Dept. Elect. Eng., Aalborg Univ., Aalborg, Denmark, 2009.
14. W. Novotny and T. A. Lipo, Vector Control and Dynamics of AC Drives. Oxford, U.K.: Clarendon, 1996.
15. H. Siegfried Heier, Grid Integration of Wind Energy Conversion Systems. Chichester, U.K.: Wiley, 2009.
16. S. Morimoto, H. Nakayama, M. Sanada, and Y. Takeda, "Sensorless output maximization control for variable-speed wind generation system using IPMSG," IEEE Trans. Ind. Appl., vol. 41, no. 1, pp. 60–67, Jan./Feb. 2005.
17. Linden and T. B. Reddy, Handbook of Batteries, 3rd ed. New York, NY, USA: McGraw-Hill, 2002.
18. Voltage Characteristics of Electricity Supplied by Public Electricity Networks, Std. NE 50160, 2010.
19. Z. M. Salameh, M. A. Casacca, and W. A. Lynch, "A mathematical model for lead-acid batteries parallel," IEEE Trans. Energy Convers., vol. 7, no. 1, pp. 93–98, Mar. 1992.
20. Mirecki, X. Roboam, and F. Richardeau, "Architecture complexity and energy efficiency of small wind turbines," IEEE Trans. Ind. Electron., vol. 54, no. 1, pp. 660–670, Feb. 2007.

Published By:
Blue Eyes Intelligence Engineering
& Sciences Publication Pvt. Ltd.